Impurity-induced grain-boundary embrittlement: A simple three-dimensional model

Gastón Martínez*
Departamento de Física, Facultad de Ciencias, Universidad de Chile, Casilla 653, Santiago, Chile, and Facultad de Física, Universidad Católica de Chile, Casilla 6177, Santiago 22, Chile

Miguel Kiwi
Facultad de Física, Universidad Católica de Chile, Casilla 6177, Santiago 22, Chile
(Received 16 January 1990; revised manuscript received 17 May 1990)

The impurity-induced grain-boundary decohesion is investigated on the basis of a three-dimensional-model calculation. The grain boundary is simulated by self-consistently modifying the hopping integrals between two neighboring grains and the impurities segregated there. We find that, for a wide range of parameter values, grain-boundary decohesion does occur.

I. INTRODUCTION

Abundant experimental evidence[1-4] indicates that a certain class of impurity atoms tends to segregate to the vicinity of the grain boundaries (GB) of metals. This segregation generates a decrease of the cohesive strength and causes the boundary to be the lowest path for crack propagation, a phenomenon known as *temper embrittlement.*

This phenomenon has received much attention from the engineering point of view. The embrittling elements are well known and the effects they induce upon alloying with most of the relevant metals have been well established.[5-7] The major outstanding task, from the applications point of view, is to find ways to effectively eliminate, or at least control, the problem.

Obviously embrittlement is a complex phenomenon, with at least two major possible origins,[5] electronic charge rearrangement in the neighborhood of GB's and the presence of interlocking dislocations in interaction with it. It is generally accepted that impurity segregation embrittles GB's if the interfacial surface energy is decreased (see Ref. 5 and papers cited therein), by reduction of both the cohesive energy and the plastic work that accompanies fracture. The relative importance of these factors is still open to debate.

On the other hand, an explanation for intergranular fracture based on the blocking of dislocations by platelike carbide precipitates, which produce large pileups, has also been put forward.[5] Since the boundaries are weakened by the segregated impurities, the pileups initiate an intergranular crack before yielding occurs in the next grain. However, in this paper we restrict our efforts to the investigation of the electronic contribution to the embrittlement phenomenon.

From a more basic materials-science point of view, the problem is just now being studied in detail. In fact, only recently several fully quantum-mechanical models to explain this harmful phenomenon have been put forward. Using the local electron density functional Smith and Ferrante[8] evaluated quite accurately the energy of a pure GB. Lanoo[9] showed that is it possible to calculate the atomic relaxations in the vicinity of a GB, which is important in the determination of the interface topology.

An alternative approach is to use a finite cluster model, which includes grain boundaries, both with and without segregated impurities. Using this technique Briant and Messmer,[10] in a pioneer work, were able to show that when a strong embrittler is added to a metallic cluster (in their case, eight atoms forming a regular polyhedron), electric charge is always drawn from the metal atoms onto the impurity. Thus, the metal-impurity bond can be characterized as rather heterpolar of ionic. As a result of this feature of the bond, and its consequent charge transfer, less charge remains available for the neighboring metal-metal bonds, which weakens them considerably.

Along this line Eberhart and Vvedensky[11] established that the appearance of localized electronic states on the GB provides a reliable indication of intergranular temper embrittlement in polycrystalline materials. Goodwin *et al.*,[12] in a very recent contribution, reported on a total-energy pseudopotential calculation of a large super cell (eighteen atoms arranged in six layers). They evaluated the energy required to fracture a sample along a GB with impurities, and also the energy necessary to separate two consecutive metallic layers in the vicinity of a GB. Finally, they compared these results with the energy required to fracture a pure metal, to find that in both cases the interlayer cohesion is enhanced by the presence of impurities.

However, there is still much to be learned from simple infinite models of the GB, treated within the tight-binding approximation. Gonçalvez da Silva[13] computed the electronic band structure of an infinite GB, without impurities, but allowed the position of the atoms on the GB to relax. He found that a band of localized states formed above the Fermi level. Along similar lines we recently[14] used a one-dimensional model to show that, for a wide range of values of the parameter space, localized states also form below the Fermi level. The existence of these localized levels implies, for some parameter values, a reduction of the cohesive strength between metal layers adjacent to the GB. This is in agreement with the conjecture of Briant and Messmer[10] and with a semiqualitative

model by Losch,[15] based on cohesive energy arguments of small molecules. Villaseñor *et al.*[16] also studied a one-dimensional GB, from the energetics point of view, employing the Hellman-Feynman theorem. They found localized states on the GB and possible GB decohesion.

Thus, it is clear from both experiment and theory that the segregation of impurities to the grain boundaries induces important changes of the physical behavior of metals and of the electronic density in the GB neighborhood. Thus, a systematic study of the electronic properties of the GB, and its interaction with the rest of the solid, may provide a better understanding of several phenomena and the underlying mechanisms which drive them.

This paper is organized as follows. In Sec. II we formulate a simplified three-dimensional model of the GB, which nevertheless incorporates the main ingredients required to properly characterize it. In Sec. III we derive and analyze the electronic density of states and the charge rearrangement in the neighborhood of the GB. In Sec. IV the technique to evaluate the interlayer cohesion energy is presented and implemented, and finally in Sec. V conclusions are drawn.

II. THE MODEL

A planar GB breaks the translational invariance along the direction perpendicular to it. This gives rise to strongly localized electronic states in the neighborhood of the GB, especially when segregated impurities are also present. On the other hand, a fair amount of information on the topology of the GB itself, and on the positions adopted by the GB impurities, does exist.[17] We can summarize this information as follows: (a) The GB is always quite narrow, and most of the time just a single atomic layer thick; (b) while the exact atomic positions in the GB are unknown, the interface retains crystal structure even at nonzero temperatures. However, according to molecular-dynamics results,[18] the melting temperature of the GB is lower than the bulk one; and (c) for a wide variety of GB's the two-dimensional periodicity is commensurate (in fact, most of the time identical) on both sides of the boundary; these are called symmetric tilt boundaries.

The most embrittling, or harmful, impurities that segregate towards the GB are phosphorus and antimony in commercial steels and sulfur in nickel and nickel alloys. The outer unfilled shells of these impurities adopt similar electronic configurations and have a strong tendency towards forming covalent bonds with transition-metal atoms. From chemisorption model calculations[19] a tendency of this type of impurity to form bridges between two metal atoms is inferred. However, it is also possible that the $3p$ impurity electrons hybridize with the $3d$ metal states, to form a special band localized on the GB. In both the above-mentioned cases the electronic states on the GB generate bands which differ from the pure metal ones. This difference will, of course, depend on the impurity concentration and on its spatial distribution.

Our model intends to incorporate all the above-mentioned features, while at the same time using as few parameters as possible. Thus, we start adopting a high-symmetry system, with a well-known solution, and introduce the GB as a local perturbation. This way, standard Green's function and perturbation theory techniques can be used to compute the relevant quantities.

Due to the severe complications associated with a realistic GB we model it, in close analogy to Goodwin *et al.*,[12] as a layer on which the translational invariance of the lattice is broken. The segregated impurities distribute themselves on this layer, either forming a superstructure or at random. While this constitutes drastic simplifications, it rescues the essential elements of the interface and allows us to derive qualitative results.

To define the model analytically we assume a simple cubic lattice, to represent the pure transition metal, and incorporate the GB as a local perturbation. The cohesive energy of transition metals strongly depends on the degree of $3d$-band filling. On the other hand, their electronic structure is quite similar over the whole series; only the Fermi energy varies from element to element. Thus, in order to simplify the calculations we just retain a single s-like orbital per atom. The unperturbed Hamiltonian can consequently be written as

$$\hat{\mathbf{H}}_0=\sum_i \varepsilon_0|i\rangle\langle i|-\sum_i\sum_h t_{i,i+h}(|i\rangle\langle i+h|+|i+h\rangle\langle i|)\ , \tag{2.1}$$

where ε_0 is the energy of the Wannier orbital $|i\rangle$, centered on site $\mathbf{R}_i$, t_{ij} is the hopping integral between sites $\mathbf{R}_i$ and $\mathbf{R}_j$, and h runs over nearest-neighbor sites only. The two-dimensional translational invariance allows us to use the mixed Bloch-Wannier representation

$$|\mathbf{K},l\rangle=\frac{1}{(N_xN_y)^{1/2}}\sum_{\mathbf{L}} e^{i\mathbf{K}\cdot\mathbf{L}}|\mathbf{L},l\rangle\ , \tag{2.2}$$

where $\mathbf{L}$ are vectors in the plane perpendicular to the z direction, i.e., $\mathbf{R}=\mathbf{L}+l\hat{\mathbf{k}}$, $\mathbf{K}$ are pseudomomentum vectors defined by $\mathbf{K}=k_x\hat{\mathbf{i}}+k_y\hat{\mathbf{j}}$ which lie in the first square Brillouin zone (FSBZ). A straightforward calculation allows us to cast the original Hamiltonian into a sum of $\mathbf{K}$-dependent ones:

$$\hat{\mathbf{H}}_0=\sum_{\mathbf{K}}\hat{\mathbf{H}}_0(\mathbf{K})\ , \tag{2.3a}$$

where

$$\hat{\mathbf{H}}_0(\mathbf{K})=(\varepsilon_0+\Lambda_{\mathbf{K}})\sum_l|\mathbf{K},l\rangle\langle\mathbf{K},l| - \sum_l t_{l,l+1}(|\mathbf{K},l\rangle\langle\mathbf{K},l+1|+\text{H.c.})\ . \tag{2.3b}$$

Above, $t_{l,l+1}$ is the hopping between sites belonging to two contiguous layers, which for the unperturbed system are assumed to be all the same, independent of site. We will refer to this as the metal-metal MM hopping matrix element t_{MM}. This way $\Lambda_{\mathbf{K}}$ becomes

$$\Lambda_{\mathbf{K}}=-2t_{MM}[\cos(k_xa)+\cos(k_ya)]\ , \tag{2.4}$$

where a is the transition-metal interatomic distance. The $\mathbf{K}$-dependent Hamiltonian (2.3b) is isomorphic with a

pure infinite one-dimensional chain Hamiltonian.

Starting from the Greenian operator

$$\hat{\mathbf{g}}(z,\mathbf{K})=[z-\hat{\mathbf{H}}_0(\mathbf{K})]^{-1}\ , \tag{2.5}$$

it is easy to obtain the Green's functions for each $\mathbf{K}$ as the following matrix element:

$$g_{lm}(z,\mathbf{K})=\langle \mathbf{K},l|[z-\hat{\mathbf{H}}_0(\mathbf{K})]^{-1}|\mathbf{K},m\rangle\ , \tag{2.6}$$

which leads to

$$g_{ll}(z,\mathbf{K})=g_0(z,\mathbf{K})=\frac{\mathrm{sgn}(E-\Lambda_{\mathbf{K}}/2t_{MM})}{(z_{\mathbf{K}}^2-1)^{1/2}}\ , \tag{2.7}$$

and

$$g_{lm}(z,\mathbf{K})=g_0\lambda^{|l-m|}(z,\mathbf{K})\ , \tag{2.8}$$

where

$$\lambda(z,\mathbf{K})=-z_{\mathbf{K}}+\mathrm{sgn}(E-\Lambda_{\mathbf{K}}/2t_{MM})(z_{\mathbf{K}}^2-1)^{1/2}\ , \tag{2.9}$$

and

$$z_{\mathbf{K}}=E-\Lambda_{\mathbf{K}}/2t_{MM}+i0^+\ . \tag{2.10}$$

From now on, and throughout this paper, we choose $2t_{MM}=1$ as our unit of energy.

To obtain the Green's function in real space, it is necessary to integrate over the FSBZ. To do so we have used the method developed by Cunningham,[20] details of which will be discussed in the next section.

We represent the presence of impurities in the GB as an $M_{1-x}I_x$ two-dimensional substitutional alloy, of impurity concentration x, and assume that the GB retains the translational symmetry of the pure metal. All electronic effects induced in the GB will reflect on its *effective* electronic band structure. Choosing a (100) monolayer perpendicular to the z direction, and using the already-defined mixed Bloch-Wannier basis for the electron states, we introduce a GB in the pure crystal by means of the following local perturbation:

$$\hat{\mathbf{V}}_{bg}(\mathbf{K})=\tilde{\varepsilon}_I(\mathbf{K})|\mathbf{K},0\rangle\langle\mathbf{K},0| +\Delta t_1(|\mathbf{K},0\rangle\langle\mathbf{K},1|+|\mathbf{K},0\rangle\langle\mathbf{K},-1|+\mathrm{H.c.})\ , \tag{2.11}$$

where $\Delta t_1=(1-t_{IM}/t_{MM})/2$, and

$$\tilde{\varepsilon}_I(\mathbf{K})=\varepsilon_I-\Lambda_{\mathbf{K}}\frac{1-t_{II}/t_{MM}}{2t_{MM}}\ . \tag{2.12}$$

The first term in Eq. (2.11) changes the host metal orbital energy by the impurity effective orbital energy, and also changes the lopping matrix elements t_{MM} by the effective II hoppings, t_{II}, for all the atoms belonging to the layer (our GB). The second term alters the MM hoppings, which connect layer 0 to layers 1 and -1, replacing them by new IM hoppings.

To find the perturbed Green's functions we use a method developed previously,[21] which is based on the transfer-matrix technique. If we define the Greenian operator for the perturbed Hamiltonian as

$$\hat{\mathbf{G}}(z,\mathbf{K})=\{[z-\hat{\mathbf{H}}_0(\mathbf{K})-\hat{\mathbf{V}}_{bg}(\mathbf{K})]\}^{-1} \tag{2.13}$$

we obtain

$$G_{00}(z,\mathbf{K})=\frac{1}{[z_{\mathbf{K}}+t_1^2\lambda(z_{\mathbf{K}})-\tilde{\varepsilon}_I]}\ , \tag{2.14}$$

$$G_{0m}(z,\mathbf{K})=\lambda^{|m|}(z_{\mathbf{K}})t_1G_{00}(z_{\mathbf{K}})\ , \tag{2.15}$$

$$G_{mm}(z,\mathbf{K})=g_0(z_{\mathbf{K}})[1-\lambda^{|2m|}(z_{\mathbf{K}})] +t_1^2\lambda^{|2m|}(z_{\mathbf{K}})G_{00}(z_{\mathbf{K}})\ , \tag{2.16}$$

and

$$G_{m,m+1}(z,\mathbf{K})=\lambda(z_{\mathbf{K}})G_{mm}(z,\mathbf{K})\ , \tag{2.17}$$

for $m=\pm1,\pm2,\pm3,\ldots$ Above $t_1=t_{IM}/t_{MM}$.

From the Green's functions of Eqs. (2.14)–(2.17) the local density of electronic states (LDOS) and the electronic occupancy, denoted by $\rho_l(E)$ and n_l, respectively, are readily obtained. This way we evaluate the charge profiles around the interface, for different GB and host parameter values.

The measured impurity concentration on the GB depends both on the host and impurity chemical species. It lies in the range between 10 and 45 %. This is 10^5 times larger than the host impurity concentration,[22] and sufficient to change significantly the electron density in the GB region. The magnitude and sign of the change depend, in addition to the impurity concentration, on the spatial impurity distribution, which may be random or ordered.

The random impurity distribution is described by the Lloyd model for Lorentzian diagonal disorder.[23] It implies a distribution of the energy eigenvalues of the GB atoms, which are used in the evaluation of the corresponding Green's functions, the center of which is obtained self-consistently. For the mean width we adopt the difference between this self-consistent level and the host one.

For ordered impurity distributions we assume an *effective* pseudoatom for all sites on the GB layer. This pseudoatom is characterized by an effective atomic level plus an effective hopping. From now on we will simply call this pseudoatom, impurity. Its atomic level is evaluated self-consistently by imposing the condition of total charge neutrality. Finally, for the II hopping we adopt, in our numerical calculations, values which reproduce the two-dimensional bandwidth in two perfectly ordered cases: the binary superstructure and the fully segregated configuration of the GB. They correspond to attractive and repulsive interactions between the metallic and insulating ions of the GB, respectively.

To evaluate the impurity atomic level, ε_I, we use Friedel's sum rule,[24] which for this case takes the form

$$10\int_{-\infty}^{E_F}\Delta\rho(\varepsilon_I,E)dE=\Delta Z\ , \tag{2.18}$$

where

$$10\int_{-\infty}^{E_F}\rho_0(E)dE=Z_M \tag{2.19}$$

defines the Fermi level for a pure host with Z_M d elec-

trons per atom. Above, $\rho_0(E)$ is the pure atom LDOS and $\Delta\rho(E)$ is the global DOS difference per atom, between the pure and the perturbed system. ΔZ is the conduction electron difference per GB atom due to the presence of impurities. The factor of 10 in Eqs. (19) and (20) takes into account the d-band degeneracy.

The self-consistency requirement on ε_I, imposed through Eq. (18), assures global charge neutrality, while allowing charge oscillations in the neighborhood of the impurity layer. These Friedel oscillations have a wavelength determined mainly by the degree of band filling, and an amplitude which decays to negligible values a few atomic lattice parameters away from the GB. The LDOS, charge transfer, and the existence of localized states in the GB will be discussed in the next section. Finally, the GB cohesion energy will be computed introducing an additional perturbation that cleaves the crystal between two consecutive layers.

III. GRAIN-BOUNDARY LDOS AND CHARGE TRANSFER

The LDOS for an atom belonging to the layer labeled by the index l and with a component $\mathbf{K}$ of the momentum parallel to the GB can be evaluated as

$$\rho_l(E,\mathbf{K}) = -\frac{1}{\pi}\mathrm{Im}G_{ll}(z,\mathbf{K})_{z=E+i0} \cdot \tag{3.1}$$

To obtain the $\mathbf{K}$-averaged LDOS, it is necessary to integrate $\rho_l(E,\mathbf{K})$ over the FSBZ to obtain

$$\rho_l(E) = \left[\frac{a}{2\pi}\right]^2 \int\int_{\mathrm{FSBZ}} \rho_l(E,\mathbf{K})d\mathbf{K} \ . \tag{3.2}$$

However, in practice, and depending both on the smoothness of $\rho_l(E,\mathbf{K})$ and the precision required, it is possible to obtain accurate results for the integral in Eq. (3.2) summing over representative high-symmetry points[20] of the FSBZ. In particular, we use a variable number of points which depends on the energy range that is being considered. For example, in the vicinity of Van Hove singularities a large number of $\mathbf{K}$ vectors is needed to obtain the required precision.

The LDOS for a pure bulk atom is known, the band edges are at $\pm 6t_{MM}$, and it has Van Hove singularities at $\pm 2t_{MM}$. When the perturbation described by Eq. (2.11) is considered, the LDOS changes principally in the metallic layers close to the GB. The magnitude of the change, and the number of neighboring layers affected, depends strongly on the GB parameters. This is especially noticeable when the latter lead to formation of band states localized on a specific layer, but which do not propagate in the direction perpendicular to the GB. This is clearly illustrated in Fig. 1, where we display the LDOS for atoms that belong to the GB (layer 0) and to the metallic layers labelled by $l=1,2$, and 3. Practically all states which are not pure metal states fade two layers away from the GB. These localized band states have, as expected, a two-dimensional character and, depending on the impurity level and the II hopping, they can split off from the band.

For each $\mathbf{K}$ value, the energy of the localized states is

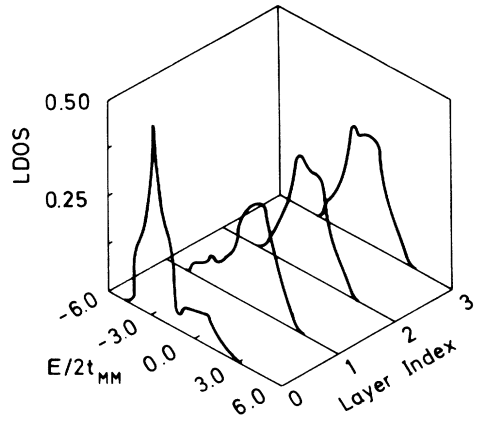

FIG. 1. Local density of electron states (LDOS) for atoms belonging to layer l. The 2D character of the GB band of localized states (layer 0) can be appreciated. Here $\frac{5}{3}t_{II}=\frac{1}{2}t_{IM}=2t_{MM}=1$ and $\varepsilon_I=-2.0$. Energies are measured in units of $2t_{MM}=1$ throughout this paper.

given by the poles of GB Green's function. If we denote these poles by $Z_{\mathbf{K}}^L$, we obtain

$$Z_{\mathbf{K}}^L = -\bar{\varepsilon}_I w \pm \mathrm{sgn}(\bar{\varepsilon}_I)\left[\bar{\varepsilon}_I^2 w^2 + \frac{t_1^4+\bar{\varepsilon}_I^2}{2t_1^2-1}\right]^{1/2} , \tag{3.3}$$

where

$$w \equiv \frac{1-t_1^2}{2t_1^2-1} \ . \tag{3.4}$$

The summation over the FSBZ $\mathbf{K}$ vectors spreads the localized states of Eq. (3.3) into a band, whose width is strongly determined by the t_{II} hopping parameter of Eq. (2.12). An impurity with $\varepsilon_I<0$ (electronegative impurity) and with a large II hopping favors electron localization in the GB layer. The IM hopping instead controls the propagation of this states into the adjacent metallic layers.

The self-consistent evaluation of the impurity energy level ε_I is based on the generalized Friedel sum rule.[24] Starting from the following generalized phase shift η,

$$\eta(z,\mathbf{K}) = \arg\det[\underline{1}-\underline{\mathbf{V}}_{\mathrm{GB}}(z,\mathbf{K})\underline{\mathbf{g}}_0(z,\mathbf{K})] \ , \tag{3.5}$$

we obtain

$$\Delta N(E_F,\mathbf{K}) = -\frac{1}{\pi}\eta(E_F,\mathbf{K}) \ , \tag{3.6}$$

where $\Delta N(E_F,\mathbf{K})$ is the total difference in occupied states induced by the peturbation. In Eq. (3.5), the perturbation and the initial Green's function are represented by the matrices $\underline{\mathbf{V}}_{\mathrm{GB}}$ and $\underline{\mathbf{g}}_0$, respectively. To obtain the total difference ΔN_{GB}, due to the presence of the GB, we sum Eq. (3.6) over a set of $\mathbf{K}$ values, as described above. Finally, the ε_I value was varied until Eq. (2.19) holds. This way, the screening of the electric potential due to the charge flow towards the GB is achieved at least in the GB itself where the charge transfer is largest.

For practically all parameter values that are different

from the pure metal ones, charge oscillations are induced in the vicinity of the GB. We define these oscillations by

$$\Delta n_l \equiv n_l - Z_\alpha \ , \tag{3.7}$$

where n_l is the occupation number of an atom belonging to the lth layer and Z_α is the corresponding atomic valence. $\alpha = M$ for all the metallic layers and I for the GB layer. For Z_I we assume an effective value given by

$$Z_I = (1-x)Z_M + x n_I \ , \tag{3.8}$$

where x is the impurity concentration and n_I is the number of electrons contributed by each impurity to the metal band. However, we have no *a priori* knowledge about the values of n_I and thus we limit ourselves to the exploration of two extreme alternatives: metallic and covalent bonding between impurity and metal atoms.

In the first case we assume that the $3p$ electrons of the impurity hybridize with the $3d$ electrons of the metal, thus forming a single band; consequently, n_I is the number of $3p$ electrons of the impurity. In the second alternative we assume a covalent MI bond formation; hence, the valence of the impurity is set equal to $-n_I$. For both these alternatives, if $Z_M > n_I$, the two-dimensional GB band holds a smaller number of electrons than the host band.

From an analytic point of view metallic and covalent bonding are closely related. In fact, all physical results that apply to the covalent case can be obtained by changing the value of Z_M to $Z'_M = Z_M + 2x n_I/(1-x)$.

In Fig. 2 we show the self-consistent impurity orbital energy level ε_I for the crystalline metallic model and for several values of $n_I = 2,3,4,5,6$. The impurity concentration x was fixed at 30% and the parameters t_{II} and t_{IM} were chosen to be equal to t_{MM}, the parent crystal hopping parameter. This way, we start with a simple model that can be compared with the realistic supercell solution of Goodwin *et al.*[12] They modeled the GB by the substitution of a percentage of metallic atoms by impurities, forming a two-dimensional superstructure on a particular layer. All the remaining parameters were kept fixed, at the parent crystal values. It is seen in Fig. 2 that $\varepsilon_I = 0$ only for $Z_M = n_I$, i.e., when no impurity is present. Two additional features can be observed in Fig. 2: The ε_I values are bound both from above and below, over the whole range of Z_M, and for all the n_I values used these curves have basically the same form, differing only in an additive constant. This is in sharp contrast with the results of by Desjonqueres and Spanjard,[24] who treated the one-impurity case in a bulk fcc transition metal and found diverging ε_I values for large $|Z_M - Z_I|$.

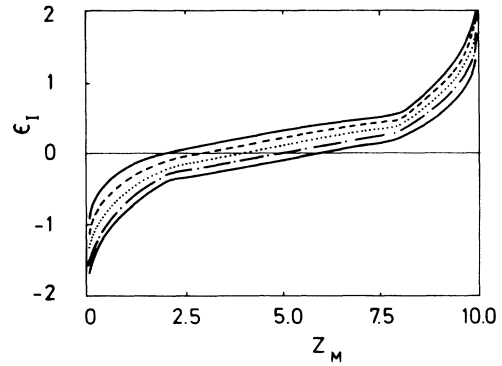

FIG. 2. Self-consistent energy levels ε_I of the GB atoms vs d-band occupation of the pure metal Z_M. For all curves $2t_{II} = 2t_{IM} = 2t_{MM}$. The upper one corresponds to $n_I = 2$ and the rest in descending order to $n_I = 3,4,5$, and 6.

The charge oscillations Δn_l versus Z_M, for $l = 0,1$, and 2, are displayed in Figs. 3(a) and 3(b). It is observed that for all values of n_I, except for $n_I = Z_M$, which corresponds to the pure crystal case, there is a charge rearrangement in which the GB and the metallic layer closest to it become oppositely charged. This implies decohesion of the system. An appreciable difference between Friedel charge oscillations induced by a single impurity and those generated by a 2D impurity layer emerges from the previous result. In particular, the wavelength of the latter seems to be of one lattice spacing in all the cases we have studied. Thus, a strong tendency to compensate the charge excess (or deficit) on the GB layer is observed, which gives rise to an opposite charge in the two layers closest to it.

The LDOS for atoms belonging to the layers $l = 0,1,2$, and 3 for $Z_M = 8$ and $n_I = 2$ is shown in Fig. 4. The local character of the perturbation is discerned, since only the GB and its two closest metallic layers are notoriously modified relative to the pure bulk DOS. The GB LDOS shows a peak below but quite close to the Fermi level, which is clear evidence of a high cohesion energy. In contrast, the neighboring layer LDOS has a smooth maximum farther below the Fermi level. These trends are confirmed in Sec. IV, in which the energy required to

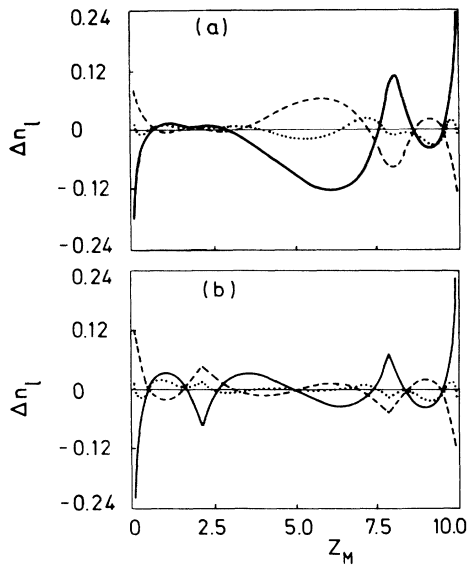

FIG. 3. Deviation from the d-electron pure metal occupation of the charge of an atom on layer l, Δn_l vs Z_M. (a) $n_I = 2$ and (b) $n_I = 5$. The solid curve corresponds to $l = 0$, the dashed one to $l = 1$, and the dotted line to $l = 2$. All other parameters are the same as in Fig. 2.

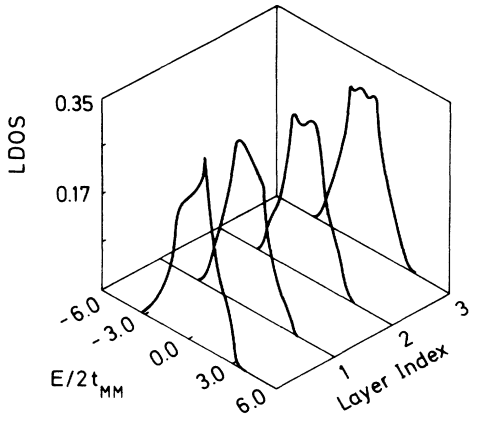

FIG. 4. LDOS for atoms on layer l. Here, $Z_M=8.0$ and $n_l=2.0$, which implies that the Fermi level is at $E_F=1.9$, in units of $2t_{MM}=1$. All other parameters are the same as in Fig. 2.

fracture the solid is explicitly evaluated.

Varying the hopping parameter t_{IM} to study the consequences of different overlaps between the effective impurity and metallic orbitals induces significant changes in the self-consistent values of ε_I [Figs. 5(a) and 5(b)], and in the charge transfer Δn_l, as displayed in Figs. 6(a) and 6(b). For $t_{IM}>t_{MM}$ the GB repels electrons if $0<Z_M<6$, and

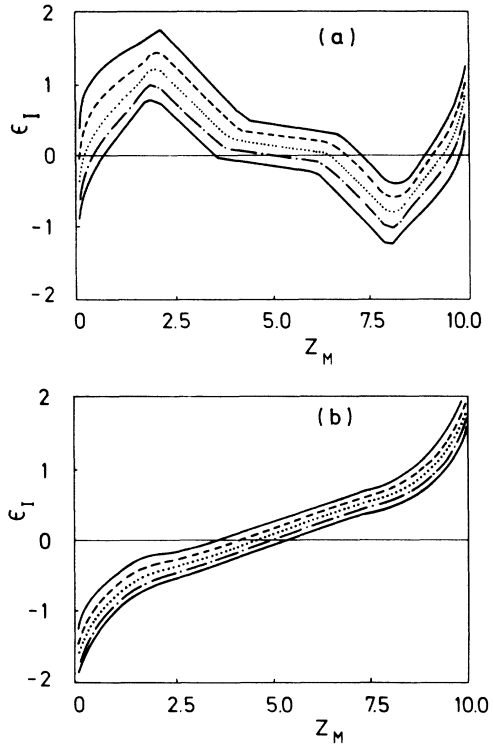

FIG. 5. Self-consistent energy levels ε_I of the GB atoms vs d-band occupation of the pure metal Z_M. The hopping parameters are (a) $2t_{II}=t_{IM}=2t_{MM}$; (b) $2t_{II}=4t_{IM}=2t_{MM}$. The upper curve corresponds to $n_I=2$ and the rest in descending order to $n_I=3,4,5$, and 6.

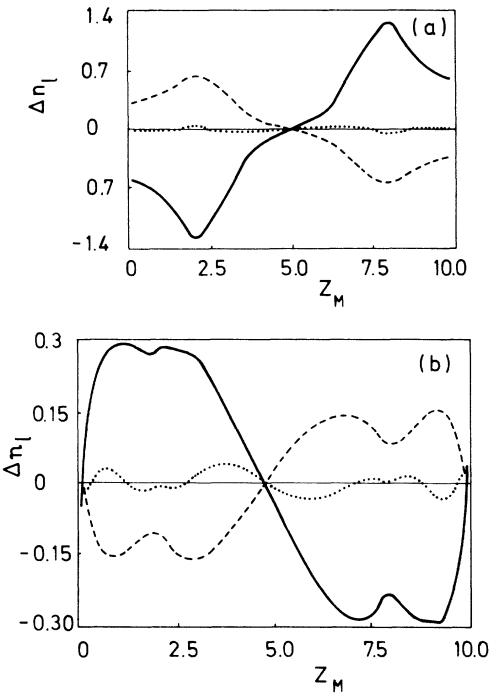

FIG. 6. Deviation from the d-electron pure metal occupation of the charge of an atom on layer l, Δn_l vs Z_M. $n_l=2$. The solid curve corresponds to $l=0$, the dashed one to $l=1$ and the dotted line to $l=2$. All other parameters are the same as in Figs. 5(a) and 5(b), respectively.

traps them if $6<Z_M<10$; the layer next to the GB shows the opposite behavior. However, the transfer in the latter case is anomalously large, particularly for energies close to the pure crystal Van Hove singularities.

This $t_{IM}>t_{MM}$ case is of special interest, since it is related to a well-known conjecture, namely that the cohesion between the GB and its nearest-neighbor layer increases at the expense of diminishing the cohesion between other parallel layers in the neighborhood of the GB.[10,19] Our results show [see Fig. 6(a)] that for $Z_M>6$ ($Z'_M>8$), an appreciable charge transfer, from the nearby metallic layers, towards the GB does occur. On the other hand, in the LDOS of Fig. 7(a) the appearance of localized states below the extended state band is quite apparent; these localized states propagate only a few layers away from the GB and are the main cause of the decohesion phenomenon. As we shall see later on, for a large region of parameter space they induce an enhancement of the cohesion between layers 0 - 1, in conjunction with a significant decrease of the 1 - 2 cohesion.

When the GB electron states are not so strongly coupled with the adjacent metallic layers, i.e., when $t_{IM}<t_{MM}$, the LDOS on the GB adopts a strongly 2D character [see Fig. 7(b)]. This implies an enhancement of the self-consistent shift of the band center and consequently the value of ε_I is larger than the one that holds in the $t_{IM}=t_{MM}$ case. However, the charge transfer exhibits two well-defined regimes: For $Z_M<5$ ($Z'_M<7$) the GB traps charge at the expense of the adjacent metallic layers; for larger values of Z_M charge is repelled by the GB.

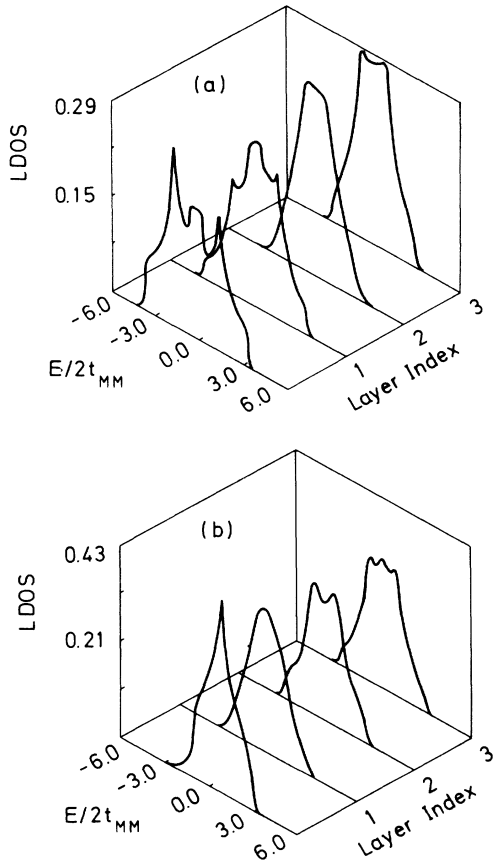

FIG. 7. LDOS for atoms on layer l. Here, $Z_M=8.0$ and $n_l=2$, which implies that the Fermi level is at $E_F=1.9$. The hopping parameters are (a) $2t_{II}=t_{IM}=2t_{MM}$; (b) $2t_{II}=4t_{IM}=2t_{MM}$.

A. GB disorder

As mentioned previously, impurities segregate towards the GB where they reach a significant concentration (up to 40%), thus substantially modifying the electronic properties of the GB neighborhood. Up to this point we have modeled these changes through the self-consistent shift of the 2D GB band center and through variations of the hopping parameter between the GB and the adjacent metal layers.

However, there are additional effects due to this large impurity concentration, mainly because of topological disorder, since impurities may locate themselves on the GB in several different ways. In fact, they may generate 2D superstructures, or segregate forming clusters, or station themselves at random. If superstructures are present, gaps will open in the alloy band structure, which are awkward to incorporate in our formalism. However, clusters or random impurity distributions induce both a broadening (or narrowing) of the 2D GB band structure and a shift of the band center. The first can be incorporated by varying t_{II} and the latter by means of Lloyd's model[23] for diagonal disorder.

We have carried out numerical calculations of the LDOS and Δn_l, in the broad GB band limit $t_{II}=2t_{MM}$, in order to understand the consequences of off-diagonal disorder. A remarkable equivalence with the charge oscillations Δn_l of the $4t_{IM}=2t_{MM}$ case is obtained, as can be seen when Figs. 6(b) and 8(a) are compared. On the other hand, the self-consistent energy ε_l and the LDOS are equivalent to the $t_{IM}=2t_{MM}$ results. The 3D LDOS shows localized states below the bulk band, but contrary to the $t_{IM}=2t_{MM}$ case of Fig. 7(a), the neighboring layers recover pure bulk characteristics faster, as can be seen in Fig. 9(a).

Analogously, for $10t_{II}=2t_{MM}$, i.e., for a narrow GB band, an equivalence with the $4t_{IM}=2t_{MM}$ case does hold for $\tilde{\varepsilon}_l$ and the LDOS, and with $t_{IM}=2t_{MM}$ for Δn_l, as can be concluded from the comparison of Figs. 6(a) and 8(b). As shown in Fig. 9(b), the LDOS exhibits 1D features which are due to the spatial anisotropy the GB electrons are subject to. The equivalences we have thus established will become relevant when the energy required to fracture the metal is evaluated, in the next section.

We now turn our attention to effects due to diagonal disorder. Following Lloyd's model we assume that the GB local self-energies $\varepsilon_{m,l}$ are distributed according to

$$P(\varepsilon_{m,l})=\frac{\Gamma}{\pi[(\varepsilon_{m,l}-\varepsilon_l)^2+\Gamma^2]}\ , \tag{3.9}$$

where m is a site index on the GB layer, l is the layer index, and ε_l and Γ are the center and the half-width of the

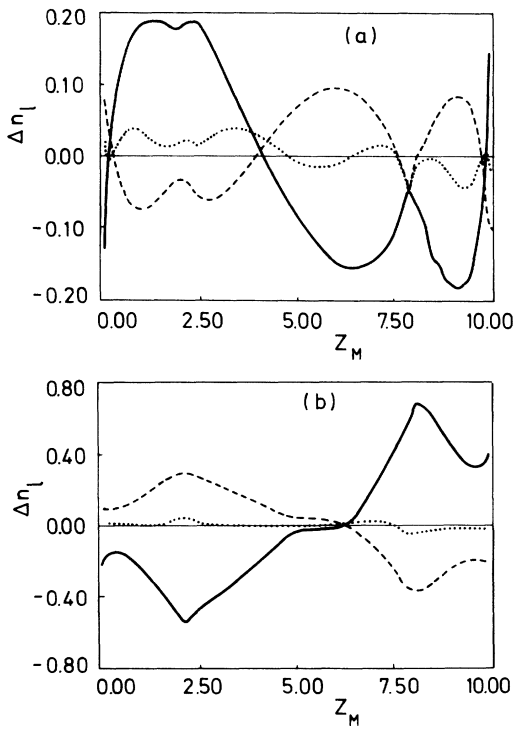

FIG. 8. Deviation from the d-electron pure metal occupation of the charge of an atom on layer l, Δn_l vs Z_M. (a) $t_{II}=2t_{IM}=2t_{MM}$, $n_l=2$, and (b) $10t_{II}=2t_{IM}=2t_{MM}$, $n_l=2$. The solid curve corresponds to $l=0$, the dashed one to $l=1$, and the dotted line to $l=2$.

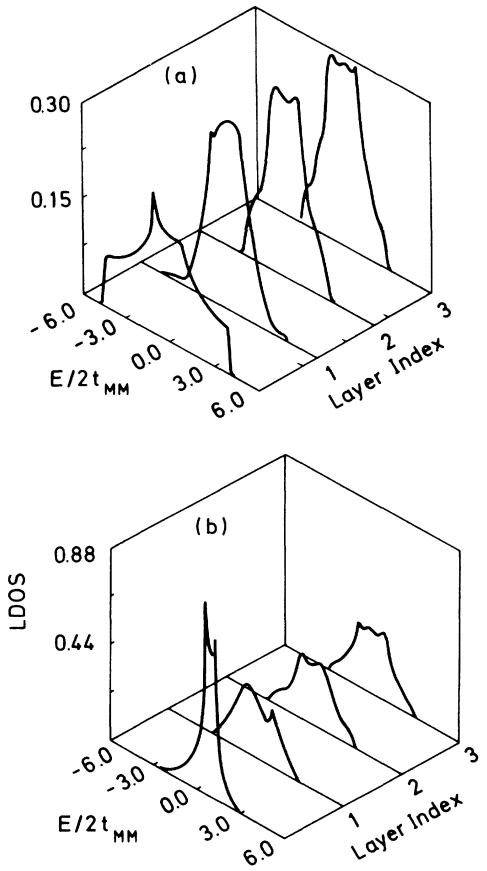

FIG. 9. LDOS for atoms on layer l. Here, $Z_M=8.0$ and $n_I=2$, which implies that the Fermi level is at $E_F=1.9$. The hopping parameters are (a) $t_{II}=2t_{IM}=2t_{MM}$; (b) $10t_{II}=2t_{IM}=2t_{MM}$.

distribution, respectively. The above expression for the distribution allows us to obtain an average Green's function of the whole crystal, including a disordered GB. Rodríguez and Weisz[25] found that the only effect of this disorder is to add an imaginary part to the **k**-dependent

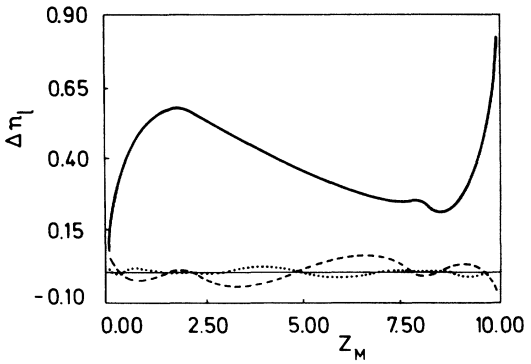

FIG. 10. Deviation from the d-electron pure metal occupation of the charge of an atom on layer l, Δn_l vs Z_M, for $2t_{II}=2t_{IM}=2t_{MM}$ and $n_I=2$. The solid curve corresponds to $l=0$, the dashed one to $l=1$, and the dotted line to $l=2$. The charge differences Δn_l were evaluated by integration of the LDOS obtained from Lloyd's model.

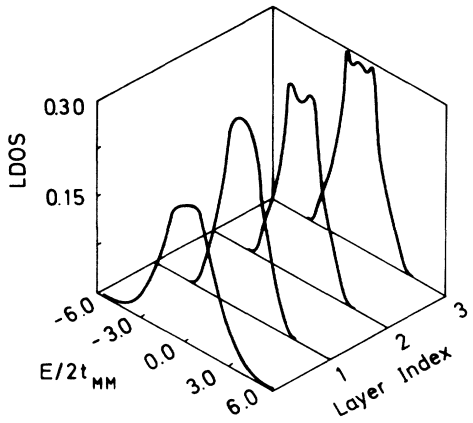

FIG. 11. LDOS for atoms on layer l. Lorentzian disorder of the energy eigenvalues of each site is assumed, centered at $\varepsilon_I=0.25$ and with a half-width $\Gamma=0.5$. The hopping parameters are $2t_{II}=2t_{IM}=2t_{MM}$, $n_I=2$, and the Fermi level is at $E_F=1.9$.

self-energy, that is

$$\tilde{\varepsilon}_I^D(\mathbf{k})=\tilde{\varepsilon}_I(\mathbf{k})-i\Gamma\ , \tag{3.10}$$

where the superscript D denotes disorder.

To illustrate this point we carried out numerical computations of the LDOS and Δn_l for the case $2t_{II}=2t_{IM}=2t_{MM}$, $\Gamma=0.5$, and taking for the center of the distribution $\tilde{\varepsilon}_I/2$. This value of $\tilde{\varepsilon}_I/2$ corresponds to one-half of the equivalent ordered case value. As shown in Fig. 10, a trapping of charge by the GB is observed over the whole range of values of Z_M. On the other hand, the LDOS of Fig. 11 shows, for the same values and $Z_M=8$, a smoothing of the singularities as a consequence of disorder, which propagates to the adjacent metallic layers.

IV. THE COHESION ENERGY

The principal objective of this contribution is the evaluation of the intergranular cohesion energy. The bulk cohesion energy of transition metals is related principally to the d orbitals, which form a narrow band of extended states in the solid. The degree of band filling determines, with few exceptions, like Mn, the degree of cohesion of the particular transition metal.[26] Thus, we assume that the GB decohesion phenomenon is mainly induced by changes in the d-band structure, which in turn originate in the presence of impurities segregated to the GB. To obtain the interlayer cohesion we evaluate the energy required to cleave the crystal between two consecutive layers, located an arbitrary distance away from the GB.

Analytically, the cleavage process is represented by the addition of a perturbation to the total Hamiltonian of the crystal, which reads

$$\hat{\mathbf{V}}_{cl}^{(l)}(\mathbf{K})=t_{l,l+1}(|\mathbf{K},l\rangle\langle\mathbf{K},l+1|+|\mathbf{K},l+1\rangle\langle\mathbf{K},l|)\ . \tag{4.1}$$

This way all the hopping terms between the layers l and

$l+1$ are eliminated, thus dividing the original infinite crystal into two semi-infinite ones, each of them with a free surface.

Using the generalized phase-shift technique introduced in Eq. (3.5)

$$\eta_{cl}^{(l)}(z,\mathbf{K})=\arg\det(\underline{1}-\underline{\mathbf{V}}_{cl}\underline{\mathbf{g}}_0)\ , \tag{4.2}$$

we obtain the cleavage energy for each $\mathbf{K}$ as[14]

$$\Delta E_{cl}^{(l)}(E_F,\mathbf{K})=\frac{1}{\pi}\int_{-\infty}^{E_F}\eta_{cl}^{(l)}(E+i0,\mathbf{K})dE\ . \tag{4.3}$$

Finally, $\mathbf{K}$ is averaged using the method of Cunningham[20] to obtain $\Delta E_{cl}^{(l)}(E_F)$. For the special case of a pure cubic crystal we obtain

$$\eta_{cl,0}(z,\mathbf{K})=\arg\left[1+\frac{z_{\mathbf{K}}}{(z_{\mathbf{K}}^2-1)^{1/2}}\right]\ , \tag{4.4}$$

which for $|z_{\mathbf{K}}|\le 1$ yields

$$\eta_{cl,0}(E,\mathbf{K})=-\tan^{-1}\left[\frac{E_{\mathbf{K}}}{(1-E_{\mathbf{K}}^2)^{1/2}}\right]\ , \tag{4.5}$$

where $E_{\mathbf{K}}=E+\Lambda_{\mathbf{K}}$ and the subscript 0 denotes the pure cubic crystal. A straightforward calculation then provides the result

$$\Delta E_{cl,0}(E_F,\mathbf{K})=\frac{1}{\pi}\left[\frac{\pi}{2}-\tilde{E}_F\sin^{-1}(E_F)-(1-\tilde{E}_F^2)^{1/2}\right]\ , \tag{4.6}$$

with the following definition of $\tilde{E}_F$:

$$\tilde{E}_F=\begin{cases}+1 & \text{if } E_F+\Lambda_{\mathbf{K}}>1\\ -1 & \text{if } E_F+\Lambda_{\mathbf{K}}<1\\ E_F+\Lambda_{\mathbf{K}} & \text{otherwise.}\end{cases} \tag{4.7}$$

To obtain the $\mathbf{K}$-averaged d-band contribution to the cohesion energy, we sum (4.6) over the special set of points on the FSBZ. The resultant $\Delta E_{cl,0}(E_F)$ is a symmetric curve with a maximum at $E_F=0$ (half-filled band) and minima at the band edges, as displayed in Fig. 12. It is important to recall that only the d-band contribution to the cohesion energy is evaluated in the context of our model. Certainly s-band effects exist and do become increasingly relevant when the d-band is either nearly empty or almost full. On the other hand, the s band, and other contributions, remain nearly constant for all the transition-metal series.[27] Consequently, the curve of Fig. 12 plus a constant term provides an adequate description of the transition-metal series cohesion energy, if magnetic effects are ignored.

When impurities are present, the generalized phase shift is given by

$$\eta_{cl}^{(l)}(z,\mathbf{K})=\arg\left[1-\frac{t_{l,l+1}^2 G_{ll}(z,\mathbf{K})\lambda(z,\mathbf{K})}{2}\right]\ , \tag{4.8}$$

where the Green's function $G_{ll}(z,\mathbf{K})$ and $\lambda(z,\mathbf{K})$ were defined in Eqs. (2.7) and (2.8), respectively. The E integral of Eq (4.3) has to be carried out numerically, which can be efficiently performed using Cunningham's method. $\Delta E_{cl}^{(0)}(E_F)$ and $\Delta E_{cl}^{(1)}(E_F)$, are the energies required to cleave the system between the GB and its nearest metallic layer (0-1 cleavage), and to cleave between the two consecutive layers closest to the GB (1-2 cleavage). To compare with the cohesion of the pure system it is convenient to define the differences

$$\delta E_{0-1}(E_F)\equiv\Delta E_{cl}^{(0)}-\Delta E_{cl,0}\ , \tag{4.9a}$$

$$\delta E_{1-2}(E_F)\equiv\Delta E_{cl}^{(1)}-\Delta E_{cl,0}\ . \tag{4.9b}$$

These differences are evaluated for the same parameter

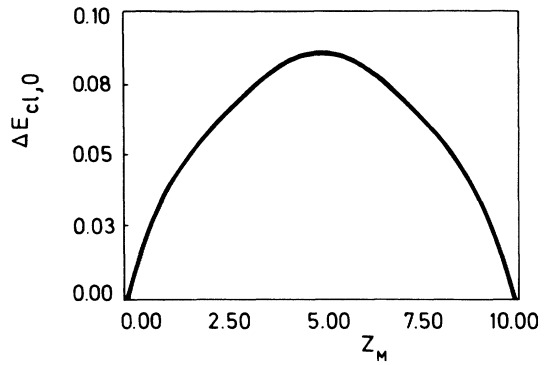

FIG. 12. Energy required to fracture a pure simple cubic crystal $\Delta E_{cl,0}$ vs the number of d electrons Z_M.

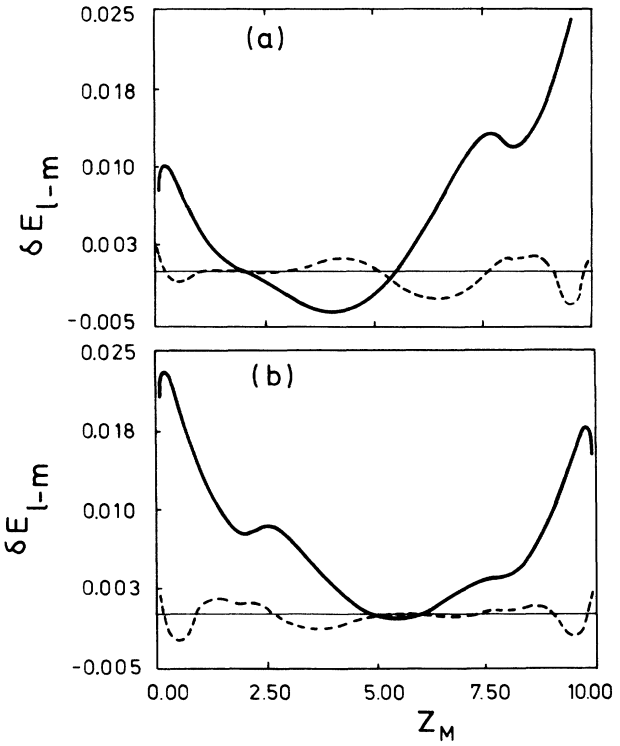

FIG. 13. Difference between the energy required to fracture the alloy and the pure crystal δE_{l-m} vs the number of d electrons of the metal Z_M. The solid line corresponds to the 0-1 and the dashed one to the 1-2 fracture, (a) to $n_I=2$, (b) to $n_I=6$. The parameters are $2t_{II}=2t_{IM}=2t_{MM}$.

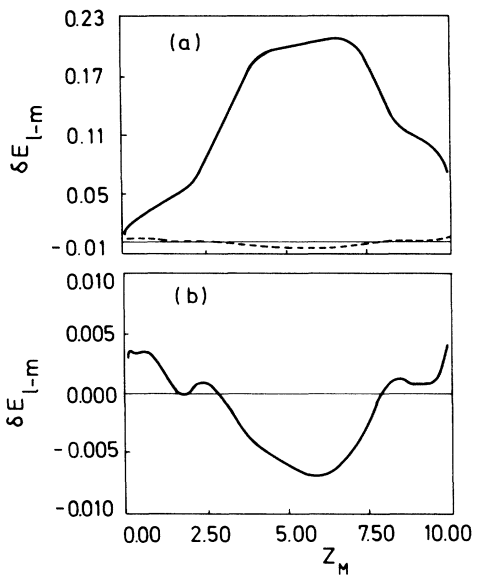

FIG. 14. Difference between the energy required to fracture the alloy and the pure crystal δE_{l-m} vs the number of d electrons of the metal Z_M. The solid line corresponds to the 0-1 and the dashed one to the 1-2 fracture. The parameters are $2t_{II}=t_{IM}=2t_{MM}$ and $n_I=2$. (b) provides an enlargement of δE_{1-2}, the dashed line of (a).

values chosen in the previous sections, in order to relate our understanding of the energy required to fracture a sample with the LDOS calculated previously. δE_{2-3} and more distant values from the GB need not be evaluated since they are negligible. The accuracy of our calculation of δE_{0-1} is of the order of 1%, obtained on the basis of dividing the FSBZ into 10 000 pieces.

The first example we have analyzed corresponds to $2t_{II}=2t_{IM}=2t_{MM}$, both for $n_I=2$ and $n_I=6$. Plots of $\delta E_{j-(j+1)}$ versus Z_M are given in Figs. 13(a) and 13(b). A significant conclusion can be drawn from the results for $n_I=2$, since they show decohesion between the 0-1 layers for $3<Z_M<5$ electrons ($5<Z'_M<7$); instead, the 1-2 bond exhibits decohesion for $6<Z_M<7(8<Z'_M<9)$. The

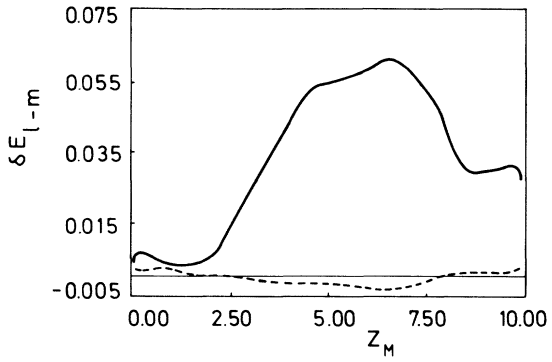

FIG. 16. δE_{l-m} vs the number of d electrons of the metal Z_M. The solid line corresponds to the 0-1 and the dashed one to the 1-2 fracture. The parameters are $10t_{II}=2t_{IM}=2t_{MM}$ and $n_I=2$.

$n_I=6$ case shows a somewhat smaller weakening than $n_I=2$, and only between layers 1-2, for $3<Z_M<4$.

In Fig. 14(a) we display plots of δE_{0-1} and δE_{1-2} versus Z_M for $2t_{II}=t_{IM}=2t_{MM}$ and $n_I=2$. An enlargement of the δE_{1-2} plot is provided in Fig. 14(b), since it illustrates an important outcome. In fact, the enhancement of the 0-1 bond, over the whole range of values of Z_M, brought about by $t_{IM}=2t_{MM}$, implies a significant reduction of the 1-2 cohesion for $3<Z_M<7$ electrons. This confirms the conjecture of Briant and Messmer[10] and of Losch,[19] that a large value of the IM bond implies a weakening of the neighboring MM one. For other values of n_I the same qualitative tendency is also observed, with slight shifts of the minimum value of δE_{1-2}.

Interesting equivalences with the preceding behavior do result when the hopping matrix element between GB atoms is adequately modified. In fact, for $t_{II}=2t_{IM}=2t_{MM}$ and $n_I=2$ one obtains, as shown in Fig. 15, results which are practically identical to adopting $4t_{II}=4t_{IM}=2t_{MM}$ and $n_I=2$. Analogously, for $10t_{II}=2t_{IM}=2t_{MM}$ and $n_I=2$ the results of Fig. 16 are obtained; their close similarity with Fig. 14 is quite remarkable.

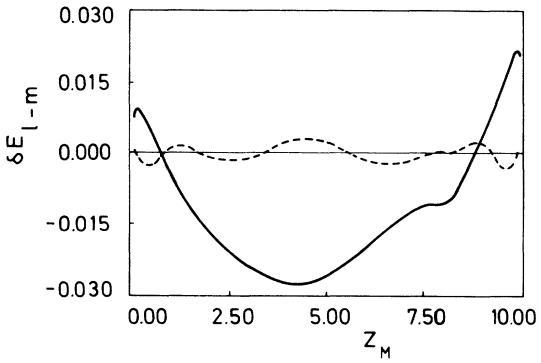

FIG. 15. δE_{l-m} vs the number of d electrons of the metal Z_M. The solid line corresponds to the 0-1 and the dashed one to the 1-2 fracture. The parameters are $t_{II}=2t_{IM}=2t_{MM}$ and $n_I=2$.

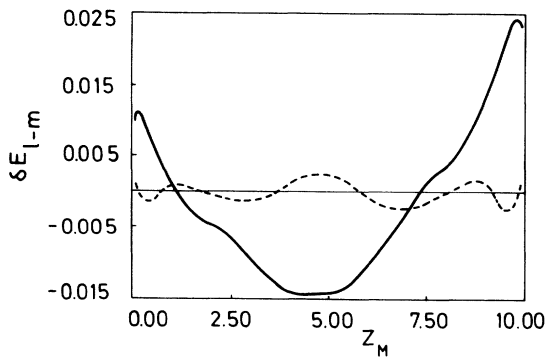

FIG. 17. δE_{l-m} vs the number of d electrons of the metal Z_M, when diagonal disorder is present. The solid line corresponds to the 0-1 and the dashed one to the 1-2 fracture. The parameters are $2t_{II}=2t_{IM}=2t_{MM}$ and $n_I=2$.

Finally, in Fig. 17 we plot δE_{0-1} and δE_{1-2} versus Z_M for the case with diagonal disorder described at the end of Sec. III. Also here a noticeable 0-1 decohesion is observed, for $2 < Z_M < 6$.

V. CONCLUSION

In order to be able to carry out our calculations, we have presented a model with several shortcomings and certain limitations. It focuses only on the electronic contribution to temper embrittlement, without incorporating effects due to dislocations. Also, both the geometry of the GB and the electronic band structure, are considerably simplified. In fact, we have treated the d band as a tenfold-degenerate s-like band. In this way, angular dependences of the d orbitals are left out. Therefore, a direct comparison of our results with experiment is not possible.

However, the calculations we were able to carry out on the basis of our model yield stable and consistent results over a wide range of parameter space. In this way, interesting qualitative inferences, which shed some light on the microscopic understanding of this complex phenomenon, were obtained. They allow us to draw general conclusions, some of which are presented below.

In order to simplify this presentation, it is convenient to recall that, within the framework of our model, it is equivalent to increase (reduce) the insulator-metal hopping parameter, t_{IM}, or to reduce (increase) the impurity-impurity one, t_{II}. Their variation induces equivalent changes on the electronic structure, and consequently on the intergranular cohesion energy. This equivalence was detailed in the two previous sections and is an important element of several models proposed to explain temper embrittlement.

For example, on the basis of semiquantiative molecular bonding arguments, Losch[19] offered several possible mechanisms to explain the intergranular embrittlement, from an electronic point of view, two of which are equivalent in our model. In fact, the first one suggests a weakening of the cohesion between the next and second-next layers to the GB (layers 1 and 2), due to the enhancement of the bond between the GB and its first neighboring layer (0-1 bond). The second suggests a reduction of the 0-1 cohesion due to the reinforcement of the bonds between the atoms on the GB, which has a significant impurity content.

The strength of the bond is mainly determined by the local electronic structure, which in turn can be understood in terms of the local density of states (LDOS). When t_{IM} is enhanced relative to t_{MM}, while $t_{II}=t_{MM}$ is kept fixed, the LDOS becomes broader and tends to localize states in the vicinity of the GB. This gives rise to a band of localized states below the pure metal energy band, as illustrated in Fig. 7(a). On the other hand, the decrease of t_{II} relative to t_{MM}, now keeping $t_{IM}=t_{MM}$ fixed, narrows the LDOS on the GB, with the consequent significant increase in the number of states with energies close to $E=0$. However, this enhancement is very localized and decays to practically the bulk value on the neighboring metal layers, as illustrated in Fig. 3. This phenomenon, known as resonance, also localizes a certain amount of states on the GB.

In the $t_{IM} < t_{MM}$ case, a localization due to a resonance inside the energy band is generated, which for our purposes makes it equivalent to the $t_{II} > t_{MM}$ case, where the localization is related to a band of localized states, i.e., to a pole of the Green's function outside of the branch cut.

Consequently, our model allows for the following possible mechanisms for the electronic contribution to temper embrittlement.

(i) A reduction of the cohesion between the first two metallic layers (layers 1 and 2) next to the GB, caused by an enhancement of the bonds between the GB and the first metallic layer in its vicinity (layers 0 and 1). This holds for metals with $3 < Z_M < 7$, as illustrated in Fig. 14, and for practically any impurity with valence between 2 and 6.

(ii) A reduction of the 0-1 cohesion due to the presence of low valence impurities ($n_I \approx 2$) in transition metals with a few d electrons (between 3 and 4) per atom. Also, a reduction of the 1-2 cohesion for the same type of impurities, but in metals with between 4 and 6 d electrons. In the same context, there is a decrease of the 1-2 bond strength for transition metals with around nine d electrons per atom, independent of the impurity valence.

(iii) A reduction of the 0-1 cohesion due to a large impurity-impurity hopping parameter. This effect is quite pronounced for the value of $t_{II}=2t_{MM}$ that we have chosen in Fig. 15, which induces decohesion for values of the atomic valence in the wide range $1 < Z_M < 8$, almost independent of the value of the impurity valence.

(iv) Finally, a reduction of the 1-2 cohesion due to the stabilization of a disordered structure of the GB, which is quite noticeable and takes place in metals with $2 < Z_M < 6$, for the parameter values of Fig. 17.

Our results yield intergranular reinforcement, as found by Goodwin *et al.*[12] but it is small in magnitude and happens only rarely, as can be seen in Fig. 13(b) for $1 < Z_M < 2$ and in Fig. 16 for $8 < Z_M < 10$, respectively. However, in most of the cases we have studied there are regions of parameter space which yield intergranular weakening, on the basis of the mechanisms detailed above.

ACKNOWLEDGMENTS

This work was supported by the Dirección de Investigación de la Universidad Católica (DIUC) and the Fondo Nacional de Ciencia y Tecnología (FONDECYT), Chile.

*Permanent address: Tecnología Integral S.A., Alameda 552, Piso 8, Santiago, Chile.

[1]*Treatise on Materials Science and Technology,* edited by C. L. Briant and S. K. Banerji (Academic, New York, 1984), Vol. 25.

[2]W. Losch, Acta Metall. **27**, 567 (1979).

[3]M. P. Seah, Surf. Sci. **53**, 168 (1975).

[4]M. Guttmann, Surf. Sci. **53**, 213 (1975).

[5]C. L. Briant and S. K. Banerji, in Ref. 1, p. 21.

[6]D. F. Stein and L. A. Heldt, in *Intefacial Segregation,* papers presented at a Seminar of the Materials Science Division of the American Society for Metals (American Society for Metals, Metals Park, OH, 1977), p. 239.

[7]R. W. Balluffi, in Ref. 6, p. 193.

[8]J. R. Smith and J. Ferrante, Phys. Rev. B **34**, 2238 (1986).

[9]A. Mauger, J. C. Bourgouin, G. Allan, M. Lanoo, A. Bourret, and L. Billard, Phys. Rev. B **35**, 1267 (1987).

[10]C. L. Briant and R. P. Messmer, Philos. Mag. B **42**, 569 (1980); and Ref. 1, p. 53.

[11]M. E. Eberhart and D. D. Vvedensky, Phys. Rev. Lett. **58**, 61 (1987).

[12]L. Goodwin, R. J. Needs, and V. Heine, Phys. Rev. Lett. **61**, 1250 (1988).

[13]C. E. T. Goncalves da Silva, Solid State Commun. **35**, 611 (1980).

[14]M. Kiwi, Gastón Martínez, and R. Ramírez, Acta Metall. **34**, 1583 (1987).

[15]E. Anda, W. Losch, N. Majlis, and E. Ure, Acta Metall. **30**, 611 (1982).

[16]P. Villaseñor-González, J. Urias, and J. L. Morán-López, J. Phys. F. **14**, 381 (1984).

[17]*Les Joints de Grains dans les Materiaux* edited by M. Aucouturier (Les Editions de Physique, Paris, 1984).

[18]V. Pontikis, in Ref. 17, p. 149.

[19]W. Losch, Acta Metall. **27**, 1885 (1979).

[20]S. L. Cunningham, Phys. Rev. B **10**, 4988 (1974).

[21]G. Martínez, J. Rössler, and M. Kiwi, Solid State Commun. **53**, 827 (1985).

[22]R. W. Balluffi, in Ref. 6, p. 200.

[23]P. Lloyd, J. Phys. C **2**, 1717 (1969); see also Ref. 27.

[24]See, for example, M. C. Desjonqueres and F. Cyrot-Lackmann, J. Phys. F **5**, 1368 (1975).

[25]D. E. Rodríguez and J. F. Weisz, Phys. Rev. B **34**, 2306 (1986).

[26]M. C. Desjonqueres and D. Spanjaard, Phys. Rev. B **35**, 952 (1987).

[27]T. Matsubara, *The Structure and Properties of Matter* (Springer-Verlag, Berlin, 1982), p. 162.